Korean J. Chem. Eng., 37(4), 597-603 (2020)
DOI: 10.1007/s11814-019-0463-z

pISSN: 0256-1115
eISSN: 1975-7220

Oxidation of Zhundong subbituminous coal by Fe^{2+}/H_2O_2 system under mild conditions

Shuai Chen, Wei Zhou, Mingjun Liu, Guangbo Zhao†, Qingxi Cao, Bojun Zhao, Kaikai Kou, and Jihui Gao†

School of Energy Science and Engineering, Harbin Institute of Technology, Harbin 150001, Heilongjiang, China
(*Received 10 May 2019 • accepted 16 December 2019*)

Abstract−Oxidation of coal under mild conditions is effective not only to understand the macromolecular network structure of coal but also to produce useful chemicals, allowing more efficient application of coal resources. In this work, the mild oxidation of Zhundong subbituminous coal (ZS) by Fe^{2+}/H_2O_2 system was carried out under various conditions, including $[Fe^{2+}]/[H_2O_2]$ molar ratio, temperature, H_2O_2 concentration and oxidation time. The liquid oxidation products were analyzed using gas chromatography/mass spectrometry (GC/MS), and the chemical structure changes were studied using Fourier transform infrared spectroscopy (FTIR). The results suggest that the oxidation efficiency of ZS with H_2O_2 is enhanced with the aid of Fe^{2+}. The optimum conditions were determined to be $[Fe^{2+}]/[H_2O_2]$ molar ratio of 0.00453, H_2O_2 concentration of 3 mol/L, 60 °C and 4 h according to the oxidation conversion rate. In total, 25 compounds were identified, which could be categorized as six group components. Most of them are valued-added chemicals, and the content of benzene carboxylic acids is the highest among them, making up 29.99% of all group components in total relative content (TRC). -CH_2- should be primary bridge connecting the aromatic rings, and alkylene chains linking three aromatic rings are abundant in ZS.

Keywords: Zhundong Subbituminous Coal, Fe^{2+}/H_2O_2 System, Hydroxyl Radicals, Mild Oxidation, Valued-added Chemicals

INTRODUCTION

Low-rank coals (LRCs) are ample fossil resources [1-4]. Currently, LRCs are widely used in combustion, gasification and pyrolysis [5-7]. However, the inherent nature of LRCs, such as high ash yield, poor thermal stability, high water content, low calorific value and easy spontaneousness, hinders the industrial application of these resources [2,8-14]. Therefore, it is necessary to exploit efficient conversion technologies which can overcome such disadvantages [8,9, 11,12,15-17]. Compared with high-rank coals, LRCs are abundant in oxygen functional groups [1,4,9], such as -OH, -COOH, -COOR, which make LRCs promising feedstocks for producing oxygenated organic chemicals [2-4,8-10,15,16,18-21]. These oxygenated organic chemicals are important chemicals in industrial manufacturing. Recently, researchers have focused on the liquid oxidation of LRCs to produce value-added chemicals as well as reveal the coal structures at the molecular level [1,2,4,11,13,14,21-29].

Oxidants, which mainly include $RuCl_3$-$NaIO_4$ [2,22,23,30-32], O_2 [18,20], NaOCl [2,4,10,16,19,25,33], and H_2O_2 [3,8,9,11,12,15,19, 21,26,34,35], are often used for oxidative transformation of LRCs. Oxidation of coal using $RuCl_3$-$NaIO_4$ can break aromatic rings of coal with high selectivity, but its industrial applications are difficult due to the high cost of $RuCl_3$-$NaIO_4$ [1,35]. O_2 oxidation of coal needs high temperature, high pressure and strong acids or alkalis [21]. Compared with other oxidants, H_2O_2 and NaOCl are low-priced, easily available, and eco-friendly [12,21,35]. However, NaOCl oxidation of coal produces large amount of chloro-substituted species, which causes difficulties both in understanding coal structures and separating liquid oxidation products [12,35]. H_2O_2 oxidation of coal cannot be involved in other elements except H and O and produces value-added chemicals; this has received wide attention from researchers.

Miura et al. found that the mild oxidation of LRCs using H_2O_2 could produce small molecule fatty acids in high yield and selectivity in 1996 [1,8]. After that, oxidation of coal with H_2O_2 was used to produce carboxylic acids, including benzene polycarboxylic acids and aliphatic carboxylic acids, and get insight into the molecular structure of coal [3,9,12,15,21,26,34,35]. Pan et al. conducted H_2O_2 oxidation of thermal extraction residue. The result showed that -CH_2CH_2- and -CH_2- were main bridged bonds between aromatic rings and benzene rings [11]. Doskočil et al. studied oxidation of South Moravian lignite using H_2O_2 under a wide range of reaction conditions. They found that for the production of succinic acid and malonic acid, the suitable condition was especially at 40 °C for 4 h and 50 °C for 4 h, respectively [3]. Liu et al. found that H_2O_2 oxidation of Xianfeng lignite-derived residue could produce polycyclic aromatic carboxylic acids and benzene carboxylic acids in high selectivity [21]. Wang et al. found that H_2O_2 oxidation of coal pitch could acquire aliphatic carboxylic acids, alkanoic acids, benzene polycarboxylic acids and a small quantity of alkylbenzenes [26]. However, researches showed that H_2O_2 had low reactivity with coal [12,35]. A large amount of H_2O_2 needed to be used to convert coal into organic chemicals as much as possible, which increased the production cost. Therefore, improving the reactivity of H_2O_2 with coal has attracted attention.

Oxidation of coal with H_2O_2 aqueous solution as oxidant is a

†To whom correspondence should be addressed.
E-mail: zhaogb@hit.edu.cn, gaojh@hit.edu.cn

free radical reaction, which hydroxyl radicals (·OH), derived from the decomposition of H_2O_2 react with coal to achieve oxidative depolymerization of coal [10,21]. Therefore, the key to enhancing the reactivity of H_2O_2 with coal is to promote the decomposition of H_2O_2 to produce ·OH. Liu et al. [12] and Wang et al. [35] found that the H_2O_2 oxidation of coal was enhanced when adding acetic anhydride to H_2O_2, mainly because peracetic acid was *in situ* generated by the reaction of acetic anhydride with H_2O_2, and then peracetic acid decomposition could produce ·OH. Except for that, metal ions can promote the decomposition of H_2O_2 to produce ·OH. In comparison to other transition metal ions, Fe^{2+} is prone to catalyzing H_2O_2 decomposition to form ·OH, as shown in Eq. (1). Fe^{2+}/H_2O_2 system was widely used to remove various industrial contaminants and dispose waste water. It can effectively oxidize polycyclic aromatic hydrocarbons, phenols and textile pollution wastewater [36]. We extended the above ideas and proposed to use the Fe^{2+}/H_2O_2 system to oxidize coal. To our best knowledge, few reports are focused on the oxidation of coal with Fe^{2+}/H_2O_2 system.

$$Fe^{2+}+H_2O_2 \rightarrow Fe^{3+}+\cdot OH+OH^- \quad (1)$$

In this work, we investigated the reaction conditions of ZS with Fe^{2+}/H_2O_2 system, including $[Fe^{2+}]/[H_2O_2]$ molar ratio, temperature, H_2O_2 concentration and oxidation time. The liquid oxidation products were separated and analyzed with GC/MS, and FTIR was used to determine the structural alteration of coal. The purpose of this work was the assessment of the possibility to obtain value-added organic chemicals and understand ZS structural features through the reaction of ZS with Fe^{2+}/H_2O_2 system.

MATERIALS AND METHODS

1. Materials

ZS was collected from Zhundong Coal Mine in Xinjiang Province, China. It was pulverized to pass through a 200-mesh sieve (<74 μm) and then dried in a vacuum oven at 80 °C for 24 h before use. The ultimate and proximate analyses of the samples are shown in Table 1. H_2O_2 (30%), $FeSO_4·7H_2O$, MnO_2, methanol, anhydrous $MgSO_4$, diethyl ether and diazomethane are analytical reagents which were purchased from Aladdin.

2. Experimental Procedure

As displayed in Fig. 1, ZS (1 g) and $FeSO_4·7H_2O$ (0-0.37 g) were added to a 100 mL three-necked spherical flask with magnetic stirring. H_2O_2 (20 mL 1-5 mol/L) was dropwise added into the mixture using a constant pressure drop funnel while stirring the mixture. The oxidation was implemented in a water bath at a predetermined temperature (30-80 °C). After the specified reaction time (1-5 h), the reaction mixture was separated by filtration to obtain filtrate

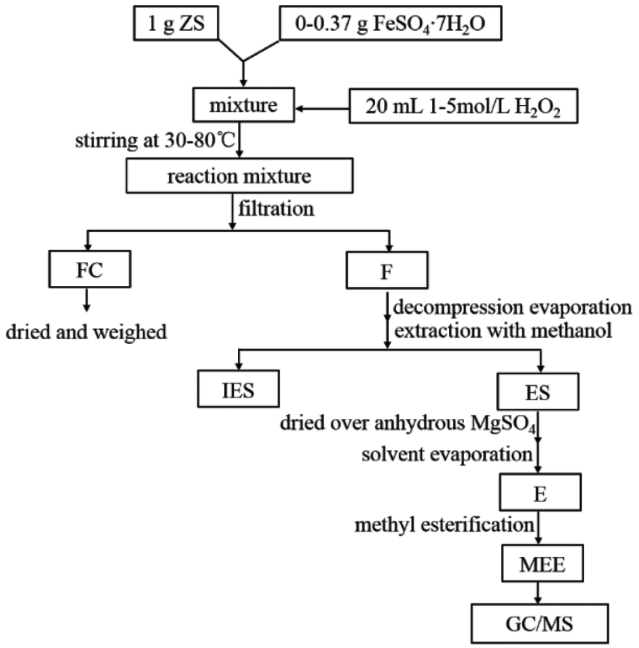

Fig. 1. Process for oxidation of ZS using Fe^{2+}/H_2O_2 system and subsequent treatments.

(F) and filter cake (FC). The remaining H_2O_2 in F was completely decomposed by adding MnO_2 [9]. MnO_2 in F was then separated through filtration. The FC was dried in a vacuum oven at 80 °C for 24 h. F was evaporated under reduced pressure and then extracted five times with 200 mL methanol to obtain extract solution (ES) and non-extractable solution (IES). ES were dried using anhydrous $MgSO_4$. When $MgSO_4·nH_2O$ was removed through filtration, the organic solvents in ES were removed through rotary evaporation to obtain extract (E). Finally, E was methylated with diazomethane in diethyl ether to obtain methyl esterified E (MEE) [1,35].

3. Analysis and Methods

3-1. Calculation Method of Oxidation Conversion Rate

To identify the optimum reaction condition, the Fe^{2+}/H_2O_2 oxidation of ZS at different oxidation times, temperatures, H_2O_2 concentrations and $[Fe^{2+}]/[H_2O_2]$ molar ratios was studied. The influence of different conditions on oxidation was studied by the oxidation conversion rate (η). η was calculated with the following formulas, as shown in Eq. (2).

$$\eta=(m_0-m_1)/m_0\times 100\% \quad (2)$$

where m_0 and m_1 are the weights of ZS and FC, respectively.

3-2. FTIR Analysis

ZS and FC were analyzed using a Nicolet 5700 FTIR spectrom-

Table 1. Proximate and ultimate analyses (wt%) of ZS

Sample	Proximate analysis (ad)				Ultimate analyses (d)				
	Moisture	Ash	Volatile	Fixed carbon	C	H	N	S	O[a]
ZS	15.87	3.71	27.36	53.06	72.50	3.56	0.69	0.49	22.76

d: dry base; ad: air dried base.

[a]By difference.

eter. KBr pellets were prepared through grinding about 1 mg of dried sample with 100 mg of KBr [26]. The frequency was 32 times per second and the accuracy was 0.01 cm^{-1}. The scanning area ranged from 4,000 cm^{-1} to 400 cm^{-1}.

3-3. GC/MS Analysis

GC/MS analysis was carried out on an Agilent 7890/5975 provided with a DB-5MS capillary column and a quadrupole mass analyzer with a split rate of 20 : 1 and a flow rate of 1.0 mL/s, operated in electron impact (70 eV) mode. The mass scan range was from 30 to 500 amu. and the electron bombardment voltage was 70 eV. The capillary column was held at 45 °C for 3 min, and then heated at 10 °C min^{-1} from 45 to 310 °C and held at 310 °C for 20 min. The data were obtained and processed using software of GC/MS, and the compounds were determined by comparing the mass spectra with NIST05 spectral library data with referring to the available reference [26]. The GC-MS peal area calculation method was adopted to determine the relative content (RC) of a compound. TRC was obtained by the sum of the RC from a class of compounds.

RESULTS AND DISCUSSION

1. Effects of Reaction Conditions

1-1. Effect of $[Fe^{2+}]/[H_2O_2]$ Molar Ratio

Fig. 2 shows the effect of $[Fe^{2+}]/[H_2O_2]$ molar ratio on oxidation conversion rate. As can be observed, the oxidation conversion rate of ZS was 22.0% in the absence of Fe^{2+} but increased when Fe^{2+} was adopted, suggesting that the oxidation efficiency of ZS with H_2O_2 was enhanced with the aid of Fe^{2+}. The reason is that ·OH plays a critical role in oxidative depolymerization of ZS using H_2O_2 aqueous solution as oxidant and H_2O_2 is easily decomposed to produce ·OH in presence of Fe^{2+} (Eq. (1)) [1,21].

When $[Fe^{2+}]/[H_2O_2]$ molar ratio was increased from 0.0029 to 0.00453, the oxidation conversion rate of coal progressively increased. The maximum oxidation conversion rate was 42.4% when the $[Fe^{2+}]/[H_2O_2]$ molar ratio was 0.00453. When the molar ratio of $[Fe^{2+}]/[H_2O_2]$ exceeded 0.00453, the oxidation conversion rate decreased with increasing Fe^{2+} dosage. This result could be due to the fact that large amount of ·OH was rapidly produced by the decomposition of H_2O_2 when $[Fe^{2+}]/[H_2O_2]$ molar ratio was relatively higher in a short time, promoting the scavenging of ·OH by the side reaction (Eq. (4)-(5)), causing the invalid decomposition of part of H_2O_2 into O_2, and thus weakening the oxidative depolymerization of ZS. According to the oxidation conversion rate, the optimum $[Fe^{2+}]/[H_2O_2]$ molar ratio is 0.00453.

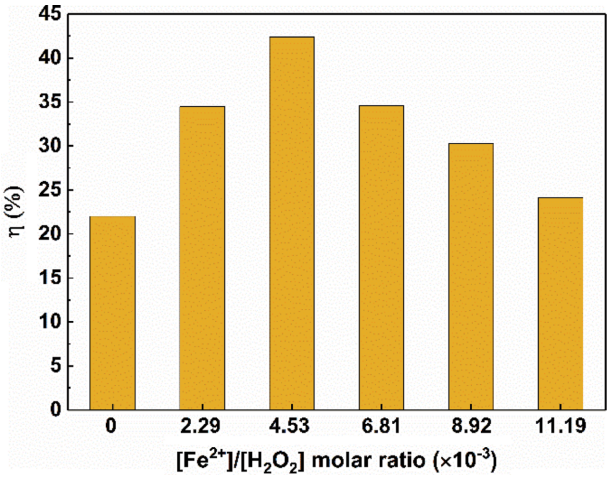

Fig. 2. Effect of $[Fe^{2+}]/[H_2O_2]$ molar ratio on oxidation conversion rate (η). Reaction conditions: oxidation time, 2 h; temperature, 60 °C; H_2O_2 concentration, 2 mol/L.

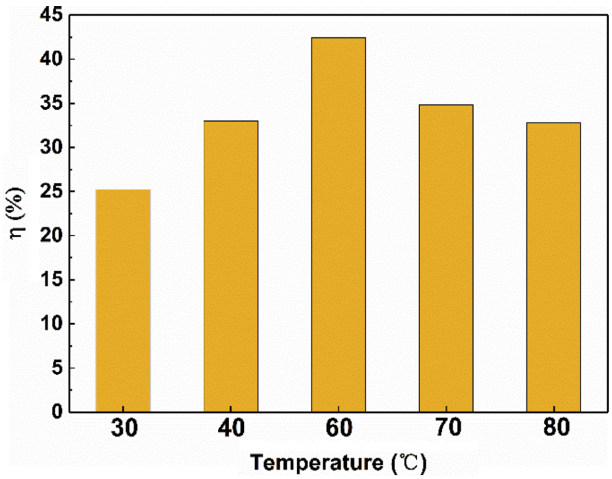

Fig. 3. Effect of temperature on oxidation conversion rate (η). Reaction conditions: oxidation time, 2 h; H_2O_2 concentration, 2 mol/L; $[Fe^{2+}]/[H_2O_2]$ molar ratio, 0.00453.

$$H_2O_2+\cdot OH \rightarrow HO_2\cdot+H_2O \quad (3)$$

$$HO_2\cdot+HO_2\cdot \rightarrow H_2O_2+O_2 \quad (4)$$

$$\cdot OH+\cdot OH \rightarrow H_2O_2 \quad (5)$$

1-2. Effect of Temperature

Fig. 3 indicates the effect of temperature on oxidation conversion rate. Temperature affects the formation rate of ·OH by Eq. (1). The higher the temperature, the faster the formation rate of OH. Therefore, as shown in Fig. 3, the oxidation conversion rate of ZS was low at low temperatures and rose with increasing temperature. When the temperature was 60 °C, the oxidation conversion of ZS increased to maximum values. However, when the temperature further increased, the oxidation conversion rate of ZS decreased. The reason for the decrease in the oxidation conversion rate could be explained in a similar way to that of the influence of $[Fe^{2+}]/[H_2O_2]$ molar ratio where the scavenging of ·OH by the side reaction (Eq. (4)-(5)) is promoted. Based on the above analysis, the suitable reaction temperature is 60 °C.

1-3. Effect of H_2O_2 Concentration

Fig. 4 reveals the effect of H_2O_2 concentration on oxidation conversion rate. The amount of H_2O_2 determines the yield of ·OH and the production cost of the entire process. It can be seen that the oxidation conversion rate increased rapidly when H_2O_2 concentration was increased from 1 mol/L to 2 mol/L. When H_2O_2 concentration rose from 3 mol/L to 5 mol/L, the oxidation conversion rate changed from 45.2% to 50.2%, suggesting that H_2O_2 concentration had a slight influence on the oxidation conversion rate

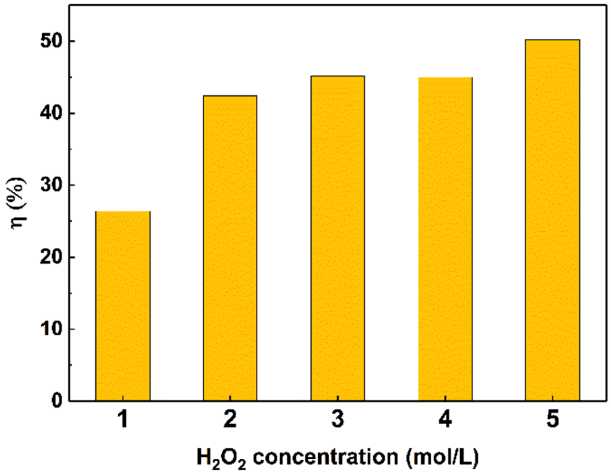

Fig. 4. Effect of H_2O_2 concentration on oxidation conversion rate (η). Reaction conditions: oxidation time, 2 h; temperature, 60 °C; $[Fe^{2+}]/[H_2O_2]$ molar ratio, 0.00453.

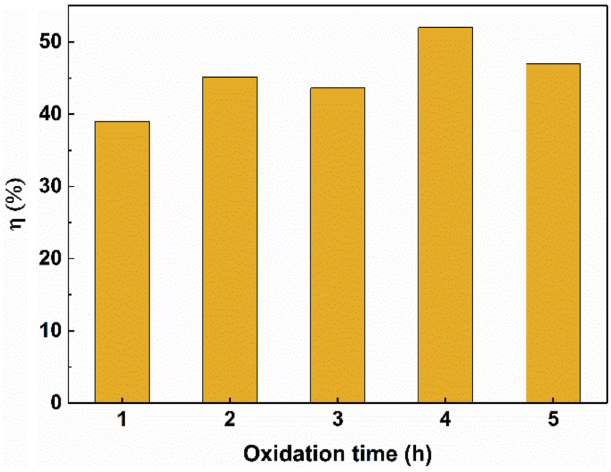

Fig. 5. Effect of oxidation time on oxidation conversion rate (η). Reaction conditions: H_2O_2 concentration, 3 mol/L; temperature, 60 °C; $[Fe^{2+}]/[H_2O_2]$ molar ratio, 0.00453.

when H_2O_2 concentration exceeded 3 mol/L. This could be explained as that the decomposition of H_2O_2 decreased because of the scavenging effect (Eq. (3)) and the regeneration of H_2O_2 (Eq. (4)-(5)) [37]. Above all, from the perspective of the oxidation conversion rate and the production cost, 3 mol/L is selected as the most proper H_2O_2 concentration.

1-4. Effect of Oxidation Time

Fig. 5 displays the effect of oxidation time on oxidation conversion rate. The oxidation conversion rate of ZS significantly varied from 38.9% to 52.0% with prolonging the reaction time from 1 h to 4 h, while further prolonging reaction time decreased to 47% at 5 h. This indicates that that the oxidative depolymerization of coal can not only convert coal into organic chemicals but also introduce oxygen-containing substances into the macromolecular structure of coal. Wang et al. [26] found that the oxidation conversion rate of coal pitch increased as reaction time varied from 2 h to 6 h, but the oxidation conversion rate of coal pitch decreased when the

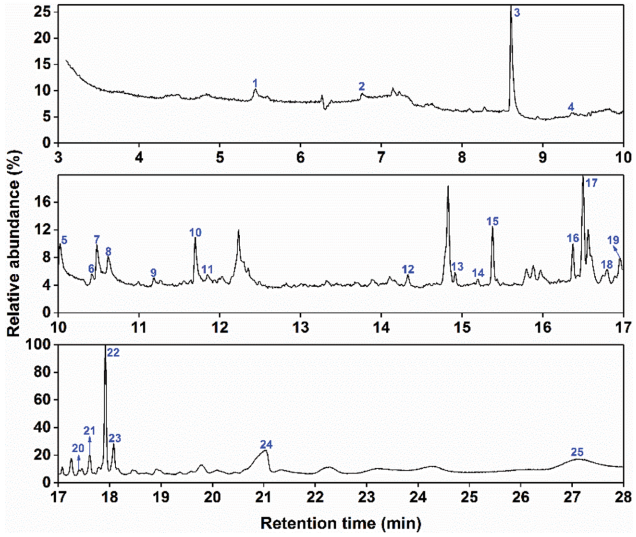

Fig. 6. Total ion chromatograms of the MEE from oxidation of ZS with Fe^{2+}/H_2O_2 system. Reaction conditions: H_2O_2 concentration, 3 mol/L; temperature, 60 °C; $[Fe^{2+}]/[H_2O_2]$ molar ratio, 0.00453; oxidation time, 4 h.

reaction time exceeded 6 h, which was consistent with ours. The oxidation conversion rate of coal is the maximum for 4 h, implying that 4 h may be the optimum oxidation time to produce organic chemicals through the reaction of ZS and ·OH· the decomposition of H_2O_2 produces in presence of Fe^{2+}.

Based on the above results, the optimum reaction conditions are $[Fe^{2+}]/[H_2O_2]$ molar ratio of 0.00453, H_2O_2 concentration of 3 mol/L, 60 °C and 4 h. The mass of FC, ES and IES produced in the optimum reaction conditions are shown in Table S2. ZS was oxidized under the optimum reaction conditions in the following discussions.

2. GC/MS Analysis

As displayed in Fig. 6 and Table 2, 25 compounds were identified in MEE by GC/MS analysis in total. Their parent products can be categorized as hydrocarbons (HCs), alkanoic acids or alkenoic acids (AAs), alkanedioic acids or alkenedioic acids (ADAs), alkanetricarboxylic acids or alkenetricarboxylic acids (ATCAs), benzene carboxylic acids (BCAs), and others species (OSs) [1,14,19, 26,27,32].

As Fig. 7 and Table 2 display, 19 carboxylic acids (CAs) were detected by GC/MS analysis, including 3 AAs, 10 ADAs, 4 ATCAs and 2 BCAs. The precursors of AAs, ADAs and BCAs are arylalkenes or arylalkanes, α,ω-diarylalkenes or α,ω-diarylalkanes and condensed aromatics [1]. Among the detected AAs, 14-methylpentadecanoic acid, which can be used to produce emulsifiers, dispersants and lubricants, is the most abundant, accounting for 22.1% of all the group components in TRC, suggesting that ZS could contain large amounts of long-chain alkyl groups. In addition, (E)-but-2-enoic acid exists in the detected AAs, which can be used to synthesize resins, plasticizers and drugs. The detected ADAs are classified into 7 alkanedioic acids (oxalic acid, malonic acid, 2-methylmalonic acid, succinic acid, 2-methylsuccinic acid, 2-methylenesuccinic acid & 2-ethylidenemalonic acid), 2 alkenedioic acids (fumaric acid & maleic acid) and 1 heterocyclic aromatic acid. Most

Table 2. Compounds detected in the product from ZS oxidation with Fe^{2+}/H_2O_2 system. Reaction conditions: H_2O_2 concentration, 3 mol/L; temperature, 60 °C; $[Fe^{2+}]/[H_2O_2]$ molar ratio, 0.00453; oxidation time, 4 h

Peak	Parent compound	Relative content/%
HC		
14	2-Butylnaphthalene	0.15
19	1,3-Dimethylnaphthalene	0.88
AA		
1 & 12	(E)-but-2-enoic acid	0.91
15	8,8-Dimethyl-5,7-dioxononanoic acid	1.16
25	14-Methylpentadecanoic acid	22.1
ADA		
2	Oxalic acid	1.31
3	Malonic acid	4.12
4	2-Methylmalonic acid	0.4
5	Fumaric acid	2.27
6 & 7	Maleic acid	1.73
8	Succinic acid	1.15
9	2-Methylsuccinic acid	0.22
10	2-Methylenesuccinic acid	1.41
11	2-Ethylidenemalonic acid	0.45
21	5-Oxotetrahydrofuran-2,3-dicarboxylic acid	4.36
ATCA		
13	Ethane-1,1,2-tricarboxylic acid	0.31
17	Propane-1,2,3-tricarboxylic acid	2.51
18	(Z)-Prop-1-ene-1,2,3-tricarboxylic acid	0.41
20	2-Hydroxybutane-1,2,3-tricarboxylic acid	1.09
BCA		
22	Terephthalic acid	20.29
23	Isophthalic acid	7.11
OSs		
16	Ethyl 2,2-dimethyl-5-oxoheptanoate	0.89
24	N,4-dimethylbenzenesulfonamide	22.18

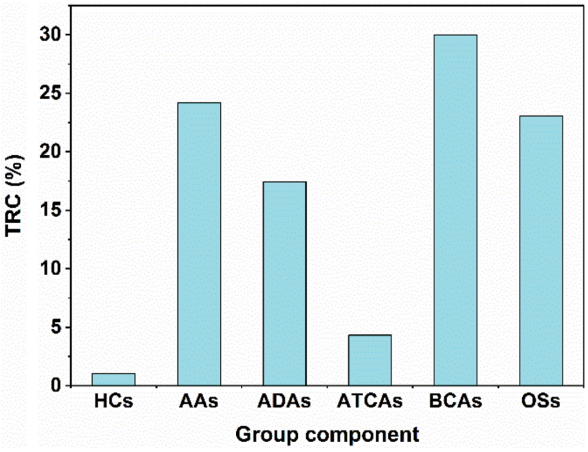

Fig. 7. Distribution of group components in the MEE from oxidation of ZS with Fe^{2+}/H_2O_2 system. Reaction conditions: H_2O_2 concentration, 3 mol/L; temperature, 60 °C; $[Fe^{2+}]/[H_2O_2]$ molar ratio, 0.00453; reaction time, 4 h.

of them are valued-added chemicals. For example, oxalic acid can be used as a complexing agent, a masking agent, a precipitating agent, a reducing agent, as a catalyst for the synthesis of phenolic resins, and as a raw material for synthetic drugs. Malonic acid can be used to synthesize perfumes, binders and pharmaceuticals. Fumaric acid is widely used in the fields of food, paint, resin and plasticizers. Malonic acid is the most abundant and the range of carbon number is from 2 to 5 in the detected alkanedioic acids, suggesting that the number of methylene connecting aromatic rings ranges from 0 to 3 and $-CH_2-$ is primary bridge connecting the aromatic rings in ZS [1,11]. The TRC of the detection of ATCAs by GC/MS analysis decreased in the order: propane-1,2,3-tricarboxylic acid>2-hydroxybutane-1,2,3-tricarboxylic acid>(Z)-prop-1-ene-1,2,3-tricarboxylic acid>ethane-1,1,2-tricarboxylic acid, suggesting that the structure of ZS contains alkylene chains linking three aromatic rings [1,12]. BCAs are the most abundant in detected compounds, accounting for 29.99% of all group components in TRC. Interestingly, the TRC of terephthalic acid is 20.29%, which is an important raw material to produce polyester resins, films, fibers and engineering plastics. Among the detected OSs, N,4-dimethylbenzenesulfonamide accounts for 22.18% of all group components in TRC, indicating that the existing forms of organosulfur species contain sulfonamides in ZS.

3. FTIR Analysis

Fig. 8 shows the FTIR spectra of ZS and FC. For FC, absorption peak at 3,791 cm^{-1} ascribed to mineral matter disappearing compared with that of ZS, suggesting mineral matter was effectively removed during the oxidation of ZS with Fe^{2+}/H_2O_2 system, which is consistent with the proximate analysis of ZS and FC (Table S1). The broad absorption at 3,000-3,600 cm^{-1} assigned to -OH groups stretching vibration of FC was stronger than that of ZS, indicating that -OH was introduced to the FC during the oxidation of ZS with Fe^{2+}/H_2O_2 system and the oxidation relativity of FC could be enhanced because of the introduced -OH [35]. Compared with FC, absorption peak at 2,800-3,000 cm^{-1} ascribed to aliphatic C-H groups stretching vibration of ZS was weak. The peaks in the 1,000-1,800 cm^{-1} belong to oxygen-containing functional groups and aromatic. Absorption peak at 1,698 cm^{-1} assigned to -COOH of FC was obvi-

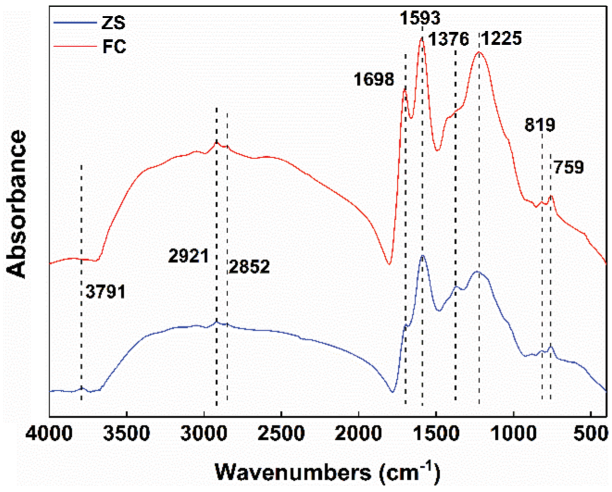

Fig. 8. FTIR spectra of ZS and FC.

ously stronger than that of ZS. The absorbance of aromatic nucleus C=C stretching vibration at 1,593 cm^{-1} of ZS and FC had a slight difference, suggesting aromatic C=C of ZS was scarcely decomposed. ZS had weaker peaks at 1,376 cm^{-1}, which is assigned to -CH_3 asymmetric deformation vibration but that of FC disappeared. The broad region at 1,100-1,300 cm^{-1} was designated as C-O stretching vibration in phenols, ethers and alcohols and had a strong absorption peak at 1,225 cm^{-1}. As displayed in Fig. 8, the absorption peak of FC at 1,100-1,300 cm^{-1} was significantly stronger than that of ZS. Comparing FC and ZS, it was observed that the absorption peak of various aromatic C-H groups out-of-plane bending vibration at 700-900 cm^{-1} had no significant change.

CONCLUSIONS

The oxidation of ZS with Fe^{2+}/H_2O_2 system was studied, the oxidation products were analyzed by gas chromatography/mass spectrometry (GC/MS), and the chemical structure changes were studied using FTIR. The main conclusions are as follows:

(1) Compared with the oxidation of ZS with H_2O_2, the catalyzed oxidation of ZS has a higher oxidation conversion rate with the aid of Fe^{2+}. The optimum conditions were determined to be [Fe^{2+}]/[H_2O_2] molar ratio of 0.00453, H_2O_2 concentration of 3 mol/L, 60 °C and 4 h based on the oxidation conversion rate.

(2) GC/MS analysis of oxidized products showed that the detected organic compounds were BCAs. -CH_2- should be primary bridge connecting the aromatic rings, and alkylene chains linking three aromatic rings are abundant in ZS.

(3) FTIR analysis of ZS and FC suggested that mineral matter was effectively removed, and -OH, -COOH and C-O were introduced into FC.

ACKNOWLEDGEMENTS

This work was supported by the National Natural Science Foundation of China (Grant No. 51776055).

SUPPORTING INFORMATION

Additional information as noted in the text. This information is available via the Internet at http://www.springer.com/chemistry/journal/11814.

REFERENCES

1. F. J. Liu, X. Y. Wei, Y. Zhu, J. Gui, Y. G. Wang and X. Fan, *Fuel*, **109**, 316 (2013).
2. Z. S. Yao, X. Y. Wei, J. Lv, F. J. Liu, Y. G. Huang, J. J. Xu, F. J. Chen, Y. G. Huang, Y. Li, Y. Lu and Z. M. Zong, *Energy Fuels*, **24**, 180 (2010).
3. L. Doskočil, L. Grasset, D. Válková and M. Pekař, *Fuel*, **134**, 406 (2014).
4. J. L. Yu, Y. Jiang, A. Tahmasebi, Y. N. Han, X. C. Li, J. Lucas and T. Wall, *Chem. Eng. Technol.*, **37**, 1635 (2014).
5. Y. Huang, W. Y. Li, G. S. Wu, J. Feng and Q. Yi, *Energy Fuels*, **31**, 12977 (2017).
6. T. Muangthongon, J. Wannapeera, S. Jadsadajerm, N. Worasuwannarak, H. Ohgaki and K. Miura, *Energy Fuels*, **31**, 11954 (2017).
7. X. P. Zhang, C. Zhang, P. Tan, X. Li, Q. Y. Fang and G. Chen, *Fuel Process. Technol.*, **172**, 200 (2018).
8. K. Miura, K. Mae, H. Okutsu and N. Mizutani, *Energy Fuels*, **10**, 1196 (1996).
9. K. Mae, H. Shindo and K. Miura, *Energy Fuels*, **15**, 611 (2001).
10. F. J. Liu, X. Y. Wei, Y. Zhu, Y. G. Wang, P. Li, X. Fan, Y. P. Zhao, Z. M. Zong, W. Zhao and Y. B. Wei, *Fuel*, **111**, 211 (2013).
11. C. X. Pan, X. Y. Wei, H. F. Shui, Z. C. Wang, J. Gao, C. Wei, X. Z. Cao and Z. M. Zong, *Fuel*, **109**, 49 (2013).
12. J. Liu, X. Y. Wei, Y. G. Wang, D. D. Zhang, T. M. Wang, J. H. Lv, J. Gui, M. Qu and Z. M. Zong, *Fuel*, **142**, 268 (2015).
13. T. M. Wang, Z. M. Zong, F. J. Liu, C. Liu, J. H. Lv, J. Liu, D. D. Zhang, M. Qu, J. Gui, X. X. Liu, X. Y. Wei, Z. H. Wei and Y. Li, *Fuel Process. Technol.*, **138**, 125 (2015).
14. F. J. Liu, X. Y. Wei, Z. M. Zong and M. H. Fan, *Energy Fuels*, **30**, 2636 (2016).
15. Z. X. Liu, Z. C. Liu, Z. M. Zong, X. Y. Wei and C. W. Lee, *Energy Fuels*, **17**, 424 (2003).
16. Y. G. Wang, X. Y. Wei, H. L. Yan, F. J. Liu, P. Li and Z. M. Zong, *Fuel Process. Technol.*, **125**, 182 (2014).
17. Z. K. Li, X. Y. Wei, H. L. Yan, Y. G. Wang, J. Kong and Z. M. Zong, *Energy Fuels*, **29**, 6869 (2015).
18. W. H. Wang, Y. C. Hou, W. Z. Wu, M. G. Niu and W. N. Liu, *Ind. Eng. Chem. Res.*, **51**, 14994 (2012).
19. F. J. Liu, X. Y. Wei, Y. Lu, Y. Qing, Y. Zhu, L. Li, J. Lv, B. Sun, X. M. Yue, Z. M. Zong and W. Zhao, *Energy sources part a-recovery utilization and environmental effects*, **35**, 1967 (2013).
20. W. H. Wang, Y. C. Hou, W. Z. Wu and M. G. Niu, *Fuel Process. Technol.*, **112**, 7 (2013).
21. F. J. Liu, Z. M. Zong, J. Gui, X. N. Zhu, X. Y. Wei and L. Bai, *Fuel Process. Technol.*, **181**, 91 (2018).
22. S. Murata, Y. Tani, M. Hiro, K. Kidena, L. Artok, M. Nomura and M. Miyake, *Fuel*, **80**, 2099 (2001).
23. Y. G. Huang, Z. M. Zong, Z. S. Yao, Y. X. Zheng, J. Mou, G. F. Liu, J. P. Cao, M. H. Ding, K. Y. Cai, F. Wang, W. Zhao, Z. L. Xia, L. Wu and X. Y. Wei, *Energy Fuels*, **22**, 1799 (2008).
24. J. H. Lv, X. Y. Wei, Y. Qing, Y. H. Wang, Z. Wen, Y. Zhu, Y. G. Wang and Z. M. Zong, *Fuel*, **128**, 231 (2014).
25. J. H. Lv, X. Y. Wei, Y. Y. Zhang and Z. M. Zong, *Fuel*, **226**, 658 (2018).
26. Y. L. Wang, X. H. Chen, M. J. Ding and J. Z. Li, *Energy Fuels*, **32**, 796 (2018).
27. F. Liu, H. Guo, Q. Wang, R. Haider, M. A. Urynowicz, P. H. Fallgren, S. Jin, M. Tang, B. Chen and Z. Huang, *Fuel*, **237**, 1209 (2019).
28. F. J. Liu, Z. M. Zong, W. T. Li, X. N. Zhu, X. Y. Wei, M. C. Tang and Z. X. Huang, *Fuel*, **242**, 883 (2019).
29. Y. G. Wang, Z. S. Niu, J. Shen, P. Li, Y. X. Niu, W. Zhao and X. Y. Wei, *Fuel Process. Technol.*, **185**, 100 (2019).
30. F. J. Liu, X. Y. Wei, J. Gui, P. Li, Y. G. Wang, W. T. Li, Z. M. Zong, X. Fan and Y. P. Zhao, *Fuel Process. Technol.*, **126**, 199 (2014).
31. J. H. Lv, X. Y. Wei, Y. H. Wang, T. M. Wang, J. Liu, D. D. Zhang and Z. M. Zong, *Rsc Adv.*, **6**, 11952 (2016).
32. Z. S. Niu, Y. G. Wang, J. Shen, Y. X. Niu, G. Liu, W. Zhao and X. Y. Wei, *Fuel*, **241**, 1164 (2019).
33. F. J. Liu, X. Y. Wei, M. H. Fan and Z. M. Zong, *Appl. Energy*, **170**,

415 (2016).
34. A. Tahmasebi, J. Yu, J. Yu, X. Li and J. Lucas, *Fuel Process. Technol.*, **129**, 213 (2015).
35. Y. G. Wang, X. Y. Wei, J. Liu, H. L. Yan, Z. H. Wei, Y. Li, P. Li, F. J. Liu and Z. M. Zong, *Fuel Process. Technol.*, **136**, 56 (2015).
36. S. Giray, M. H. Morcali, S. Akarsu, C. A. Ziba and M. Dolaz, *Sustainable Environ. Res.*, **28**, 165 (2018).
37. C. C. Jiang, Z. Gao, H. L. Qu, J. W. Li, X. X. Wang, P. Li and H. Liu, *J. Hazard. Mater.*, **250-251**, 76 (2013).

Supporting Information

Oxidation of Zhundong subbituminous coal by Fe^{2+}/H_2O_2 system under mild conditions

Shuai Chen, Wei Zhou, Mingjun Liu, Guangbo Zhao†, Qingxi Cao, Bojun Zhao, Kaikai Kou, and Jihui Gao†

School of Energy Science and Engineering, Harbin Institute of Technology, Harbin 150001, Heilongjiang, China
(*Received 10 May 2019 • accepted 16 December 2019*)

The proximate and ultimate analysis of ZS and FC are shown in Table S1. Compared with ZS, the content of moisture and ash in FC decrease, but the volatile and fixed carbon content of FC increase. The content of N and S in FC are lower than in ZS, suggesting that nitrogen-containing substances and sulfur-containing substances in ZS are removed during the oxidation of ZS using Fe^{2+}/H_2O_2 system, which is consistent with the detected compounds in MEE by GC/MS. Besides, O content in FC significantly increases compared with ZS, suggesting oxygen-containing substances increase in FC.

As shown in Table S2, the total mass of FC, ES and IES is 0.5914 g, which is less than the mass of raw coal, suggesting that part of the coal is converted into gas products during the reaction. In our ongoing work, the distribution of gas products will be investigated to better understand the oxidation mechanism.

Table S1. Proximate and ultimate analyses (wt%) of ZS and FC

Sample	Proximate analysis (ad)				Ultimate analyses (d)				
	Moisture	Ash	Volatile	Fixed carbon	C	H	N	S	O[a]
ZS	15.87	3.71	27.36	53.06	72.50	3.56	0.69	0.49	22.76
FC	10.01	1.23	31.25	57.51	63.58	3.49	0.61	0.19	32.13

d: dry base; ad: air dried base.

Table S2. FC, ES and IES produced in the optimum reaction condition. Reaction conditions: H_2O_2 concentration, 3 mol/L; temperature, 60 °C; $[Fe^{2+}]/[H_2O_2]$ molar ratio, 0.00453; oxidation time, 4 h

	FC	ES	IES
mass/g	0.4799	0.0702	0.0413